Proc. Natl. Acad. Sci. USA
Vol. 93, pp. 2795–2800, April 1996
Genetics

Regulation of meiotic chromatin loop size by chromosomal position

(synaptonemal complex/telomere/chromatin packaging/recombination/*in situ* hybridization)

HENRY H. Q. HENG*†, JOHN W. CHAMBERLAIN‡, XIAO-MEI SHI‡, BARBARA SPYROPOULOS*, LAP-CHEE TSUI‡, AND PETER B. MOENS*

*Department of Biology, York University, 4700 Keele Street, Downsview, ON Canada M3J 1P3; and ‡Department of Genetics, Hospital for Sick Children, 555 University Avenue, Toronto, ON Canada M5G 1X8

Communicated by C. C. Tan, Fudan University, Shanghai, Peoples Republic of China, November 7, 1995

ABSTRACT **At meiotic prophase, chromatin loops around a proteinaceous core, with the sizes of these loops varying between species. Comparison of the morphology of sequence-related inserts at different sites in transgenic mice demonstrates that loop size also varies with chromosomal geography. Similarly, chromatin loop lengths differ dramatically for interstitially and terminally located hamster telomeric sequences. Sequences, telomeric or otherwise, located at chromosome termini, closely associate with the meiotic proteinaceous core, forming shorter loops than identical interstitial sequences. Thus, we present evidence that different chromatin packaging mechanisms exist for interstitial versus terminal chromosomal regions, which act separately from those operating at the level of the DNA sequence. Chromosomal position plays the dominant role in chromatin packaging.**

The functional importance of the variable and reversible packaging of chromatin is drawing increasing attention in research on development, gene regulation, and cell division, both mitotic and meiotic. There are two unique features of the meiotic division: the recombination of homologous chromosomes and the segregation of chromosome sets such that haploid products are formed from diploid cells. These characteristics of meiosis may be due in part to the packaging mechanism of its chromatin.

In meiosis, the chromatin is organized on a well defined protein core, the synaptonemal complex (SC) (1, 2). In whole-mount spread preparations, measuring from core attachment to the tip of the loop, the average meiotic loop size has a species specificity ranging from 0.5 μm in the yeast *Saccharomyces cerevisiae* to 14 μm in the grasshopper *Choealtis conspersa*. Mouse and rat have intermediate loops of 3 μm (2). The mechanism that regulates such precise loop formation has yet to be elucidated.

Li *et al.* (3) reported that loops attach to the SC by means of random genomic sequences rather than specific sets of nucleotides. However, Pearlman *et al.* (4) suggested that attachment sites were enriched in sequences such as truncated LINES (long interspersed repetitive elements), SINES (short interspersed repetitive elements), and GT/CA tandem repeats. Nonetheless, since LINE and GT/CA probes give a scattered fluorescence *in situ* hybridization (FISH) signal over the entire pachytene nuclei rather than the expected localized pattern on the SC, these enriched sequences cannot act as unique attachment sites (5).

Sequence specificity, or at least signature DNA modifications, must play some role in attachment of the chromatin to the SC since prokaryotic sequences introduced into the mouse genome are not packaged into mouse-sized loops during meiosis, presumably because the required recognition signals for chromatin attachment are missing. Packaging into loops resumes, albeit at less than normal levels, when bacterial DNA is interspersed with mouse sequences (6).

In nonmeiotic cells, gene behavior varies with chromosomal geography. Genes located near the telomeres undergo position effect variegation, suggesting the existence of a distinct type of chromatin packaging at the chromosome ends, which prevents access to DNA binding proteins, resulting in repression of transcription. Ultrastructural investigations into this phenomenon have revealed differential chromatin structure at the extreme tip of the telomeres of rat and human chromosomes in which telomere-specific nucleosome array patterns indicate differential organization at this packaging level (7, 8). Such observations point to the telomere as a likely target for addressing the question of chromatin packaging. We hypothesized that the loop size could be used as a criterion for studying chromatin packaging and that the variation in loop size could be the consequence of differential packaging.

The present study uses DNA–protein codetection on wild and transgenic animals to show that loops at the chromosome ends are significantly shorter than elsewhere. Analysis of transgenic animals demonstrates that, within a organism, difference in loop size depends more on the chromosomal position of a sequence than on the sequence itself. This implies that specific chromatin packaging regulation exists for different regions of the chromosome. Thus, this paper provides evidence for the position effect of high-order structure of meiotic chromatin by illustrating differential intrachromosomal loop sizes.

MATERIALS AND METHODS

Chromosomal Localization of Insert in Transgenic Mice. *Transgenic mice.* The transgenic mice used in this study were derived from microinjection of cloned genomic DNA fragments containing the gene for the human major histocompatibility complex class I molecule HLA-B7. As described in detail elsewhere (9), line 18A was derived from microinjection of a 6.0-kb *Eco*RI/*Bam*HI DNA fragment (fragment **a**), containing the wild-type gene and 0.66 kb of 5′ and 2.0 kb of a 3′ flanking DNA. Lines 30, 47, and 50 were generated with a 6.0-kb *Eco*RI/*Bam*HI fragment (**k**) identical to fragment **a** except that it contained a 4-bp insertional mutation in a 5′ cis-active regulatory sequence (the **a** site) located at approximately −0.11 kb.

Transgenic animals with insert sizes of >20 kb were selected for study to facilitate visualization of loops. A transgenic mouse with a large inset of approximately 1000 copies of the mouse globin gene was also used to study the changes in morphology of the chromatin packaging of the foreign inserts as the chromosome progressed through the first meiotic division.

The publication costs of this article were defrayed in part by page charge payment. This article must therefore be hereby marked "*advertisement*" in accordance with 18 U.S.C. §1734 solely to indicate this fact.

Abbreviations: FISH, fluorescence *in situ* hybridization; SC, synaptonemal complex.

†To whom reprint requests should be addressed.

Determination of insertion size and copy number in transgenic strains. The copy number and DNA content of each strain's insertion was estimated by quantitative Southern blot analysis and confirmed by measurement of FISH signals on released chromatin fibers. Cultured cells from transgenic lines as well as rat and Chinese and golden hamster were harvested after hypotonic treatment and fixation in methanol and acetic acid. Fixed lymphocytes were dropped onto slides and washed with PBS. NaOH-releasing solution was dropped onto the slides, followed by physically releasing the chromatin by using the edge of a coverslip. Slides were then rinsed with fixative and air dried (10, 11).

The length of the inserts of each of the four transgenic mice was measured directly by FISH mapping on chromatin fiber with modifications (10–13).

Immunocytology. *Mitotic chromosome preparation.* For screening purposes, mitotic chromosomes were prepared for different mouse lines. Briefly, lymphocytes were isolated from the spleen and cultured at 37°C in RPMI 1640 medium supplemented with 15% fetal calf serum, 3 μg of concanavalin A per ml, 10 μg of lipopolysaccharide per ml, and 5×10^{-5} M 2-mercaptoethanol. After 44 hr, the cultured lymphocytes were treated with 0.18 mg of BrdU per ml for an additional 14 hr. The synchronized cells were washed and recultured at 37°C for 4 hr in α-MEM with thymidine (2.5 μg/ml). Chromosome slides were made by the conventional method for human chromosome preparation of hypotonic treatment, methanol and acetic acid fixation, and air drying.

Whole-mount surface spread spermatocyte nuclei. Testes of rat, Chinese and golden hamster, and two mouse strains, DBR and C57, were whole-mount surface spread as described (14). Briefly, 5 μl of testicular cell suspension in MEM was spread on 0.5% NaCl hypotonic solution (pH 7.4). Nuclei were picked up on a glass multiwell slide, fixed in 1% paraformaldehyde with 0.03% SDS (pH 8.0) 2 × 3 min, rinsed 3 × 1 min in 0.4% PhotoFlo (pH 8.0), and air dried.

Slides were washed 3 × 10 min in PBS (pH 7.4) with 10% antibody dilution buffer (ADB; 10% goat serum, 3% bovine serum albumin, 0.05% Triton X-100 in PBS). The middle wash also contained an additional 0.1% Triton X-100. Nuclei were incubated in the dark at room temperature overnight with antisera against SC core protein diluted 1:500 in ADB with 0.2 mg of sodium azide per ml. Following three washes in PBS/ADB as described above, nuclei were incubated in secondary antibody tagged with biotin for 2 hr at room temperature in the dark. Slides were washed 3 × 5 min in PBS, 2 × 1 min in water/0.1% Photo-Flo, and then air dried and processed for FISH.

Following hybridization of the DNA probe, slides were washed three times in PBS/ADB as described above and incubated for 2 hr in the dark with antibody against biotin tagged to a fluorescent probe, either fluorescein isothiocyanate or Cy5. Following 3 × 1 min washes in water and Photo-Flo, slides were mounted in Prolong Antifade (Molecular Probes Inc., Eugene, OR) with or without 4′,6-diamidino-2-phenylindole.

FISH Detection. Probes were isolated and biotinylated with dATP using the BRL BioNick labeling kit (15°C, 2 hr) (10). The procedure for FISH detection was performed according to Heng and Tsui (15). Briefly, slides were baked at 55°C for 1 hr. After RNase A treatment, the slides were denatured in 70% formamide in 2× SSC for 1 min at 70°C followed by dehydration with ethanol. Probes were denatured at 75°C for 5 min in a hybridization mixture consisting of 50% formamide, 10% dextran sulfate, and mouse C_0t I DNA and prehybridized for 15 min at 37°C. Probes were loaded on the denatured slides and hybridized overnight. Slides were washed and probes were detected and amplified.

Loop Measurement. *Serially sectioned nuclei.* Rat nuclei were fixed in 2% gluteraldehyde in PBS for 1 hr, postfixed in 2% osmium tetroxide, dehydrated through an alcohol series and propylene oxide, and embedded in Epon 812 according to Luft's 1:1 mixture. Material was serially sectioned and mounted on single-hole grids. Sections were stained in 2% uranyl acetate and lead citrate according to standard procedures.

Three-dimensional measurements were made by entering into the computer from a digitizer, the x and y coordinates of a given SC relative to fiducial marks on the micrograph. The z coordinate equalled the section thickness (a) times the section length in consecutive sections (b). The length was then calculated as

$$\Sigma_c = \sqrt{(a^2 + b^2)},$$

where a and b represent the sides of a right-angled triangle and c represents the hypotenuse (16).

Whole-mount spread nuclei. Loop size was defined as the distance from the SC/core attachment site to the tip of the average loop. Since chromatin condensation varied during meiosis, loop sizes were compared within the same time frame, usually in early prophase nuclei since these were well spread and had clear attachment sites to the protein core.

RESULTS

Nonterminal Loops. To evaluate the relevance of chromatin loop size variation, measurements were made on both intact and surface-spread nuclei. In a serially sectioned rat nucleus, the average nuclear radius was ≈5 μm with a corresponding volume of 524 μm^3. The total length of SCs based on three-dimensional measurements was 170 μm. A cylinder of 170 μm with a 1-μm radius would have a volume of 534 μm^3, suggesting an *in vitro* loop length of 1 μm. Measurements of the chromatin around the SCs also indicated a radius of 1 μm. If, however, interdigitation of the loops from adjacent chromosomes occurred, then the maximum length of a loop in the relatively intact meiotic prophase nucleus would be 2 μm. Since individual loops were not distinguishable in this type of preparation, serially sectioned nuclei were not suitable for studies on loop behavior.

This problem was circumvented by using FISH (15) and immunostaining (17) on whole-mount surface-spread nuclei (6). Loops from hypotonically treated, surface-spread rodent nuclei had an average length of 3 μm (Fig. 1*A*). The well-spread individual loops allowed the study of the behavior of particular loops at different stages of meiosis by FISH-painting reference sequences such as foreign inserts (e.g., pBR) (6) or telomeres. Nonterminal loops varied in size with respect to stage. Zygotene loops of pBR (Fig. 1*B*) were much less condensed than those of pachytene (Fig. 1*B*). Condensation relaxed somewhat at metaphase 1 (Fig. 1*C*) but never to the degree seen at the earliest meiotic stages.

At every stage of mouse meiosis, our observations indicated that, within the last micrometer of the SC, loops were reduced to approximately one-half to one-third that of interstitial loops as they approached the end of the chromosome (Fig. 1*A*, arrows). This phenomenon was observed in the majority of meiotic spreads, particularly when the ends of the core structure were defined by anti-core antibody staining. The relationship between this differential loop size and chromosomal position provided the basis for studying higher-order chromatin packaging mechanisms.

Terminal Loops. Observations that telomeres of *Mus musculus* were highly associated with the protein core (5) led us to investigate telomeric packaging behavior in other species such as Chinese and golden hamster, rat, frogs, chicken, and two strains of *Mus musculus* (C57 and DBA). Regardless of length, telomeres of these species were also closely connected to the core, suggesting that packaging at the tip of the chromosomes is highly conserved (data not shown).

Telomere sequences located at the ends of the chromosome maintained a uniform morphology throughout the first meiotic division, attaining the same degree of condensation as at mitotic metaphase, where signals were visualized as a con-

densed signal with FISH detection (Figs. 2 and 3). Since the mouse telomeres were so closely associated with the core and overall chromatin loop size is dramatically smaller toward the terminus, we hypothesized that the telomere sequences were in fact forming very small loops. In testing this hypothesis, we wished to exclude the possibility that there was insufficient available DNA to form interstitial-sized loops since mouse strain C57, used to develop our transgenic mice, had on average fewer TTAGGG repeats per chromosome (i.e., 6300) than other species tested (DBA mice, 10,100; rat, 13,000) (Table 1).

Since the number of telomere TTAGGG repeats varied between mouse strains (18), we determined the length of the telomeres of the various species by means of chromatin fiber mapping in order to compare their chromatin loop sizes (10, 13). Although the size of the telomeric FISH signal was very similar among different meiotic chromosomes within a species, the actual length of the telomere, as determined by chromatin fiber mapping, varied from chromosome to chromosome (data not shown). To determine the average length of the longest telomere, we based our measurements on the length of the 10 longest telomeres found in stretched chromatin fibers in each of 100 nuclei from two animals (50 nuclei per animal) (Fig. 2*A*).

Within the tested species, the shortest telomeres in terms of numbers of base pairs were those of the hamster (29 kb) (Fig. 3 *B* and *D*) and mouse strain C57 (40–50 kb) (Fig. 2*E*). Rat (78 kb; Fig. 2*C*) and DBA mouse (67 kb; Fig. 2*D*) telomeres were at least twice as long. These data are summarized in Table 1.

The highly condensed FISH signal of the terminal regions indicated that a considerable number of kilobases could be packed into the same small area. The telomere of the DBA mouse was 1.6 times more condensed than that of mouse C57 and twice as tightly packed as the hamster telomere. Similarly, rat telomeres were 2.5 times more compact than those of hamster. The fact that all telomeric chromatin formed the same small loops regardless of the copy number supported our conclusion that there existed enough TTAGGG sequences to form interstitial-sized loops. Thus, the small loops at the chromosome is not due merely to the number of DNA base pairs.

Chromosome Geography and Chromatin Packaging. Since the telomere and subtelomeric regions have reduced loop size relative to the interstitial regions, we questioned whether regulation of packaging was dependent on specific DNA sequence or on chromosomal position. Fortuitously, in the chromosomal evolution of both the Chinese and golden hamster, telomeric sequences have migrated interstitially by chromosomal fusion. Thus, we were able to compare the behavior of these interstitial telomeric sequences with their terminally located counterparts (19). The average loop length of the interstitial telomere sequences in golden hamster was 2.3 μm (Fig. 3*D*, i), similar to adjacent sequences, while the average loop length of the interstitial telomere sequences in the Chinese hamster was 5 μm (Fig. 3*B*, i). The same sequences were ultracondensed at the end of the chromosomes (Fig. 3 *B* and *D*, t). Thus, sequence was not the primary determining factor in loop size regulation.

The above observations led us to examine whether nontelomeric sequences, if moved progressively closer to the end of the chromosome, would be subject to the same packaging regulator as the telomeres. We selected four strains of chromosome C57 mice in which the same sequence had inserted at various distances from the telomere (Fig. 4*E*). These strains were denoted as lines 18A, 30, 47, and 50.

DNA fragments microinjected into mouse eggs cointegrate into the mouse chromosome as multiple copies of head-to-tail

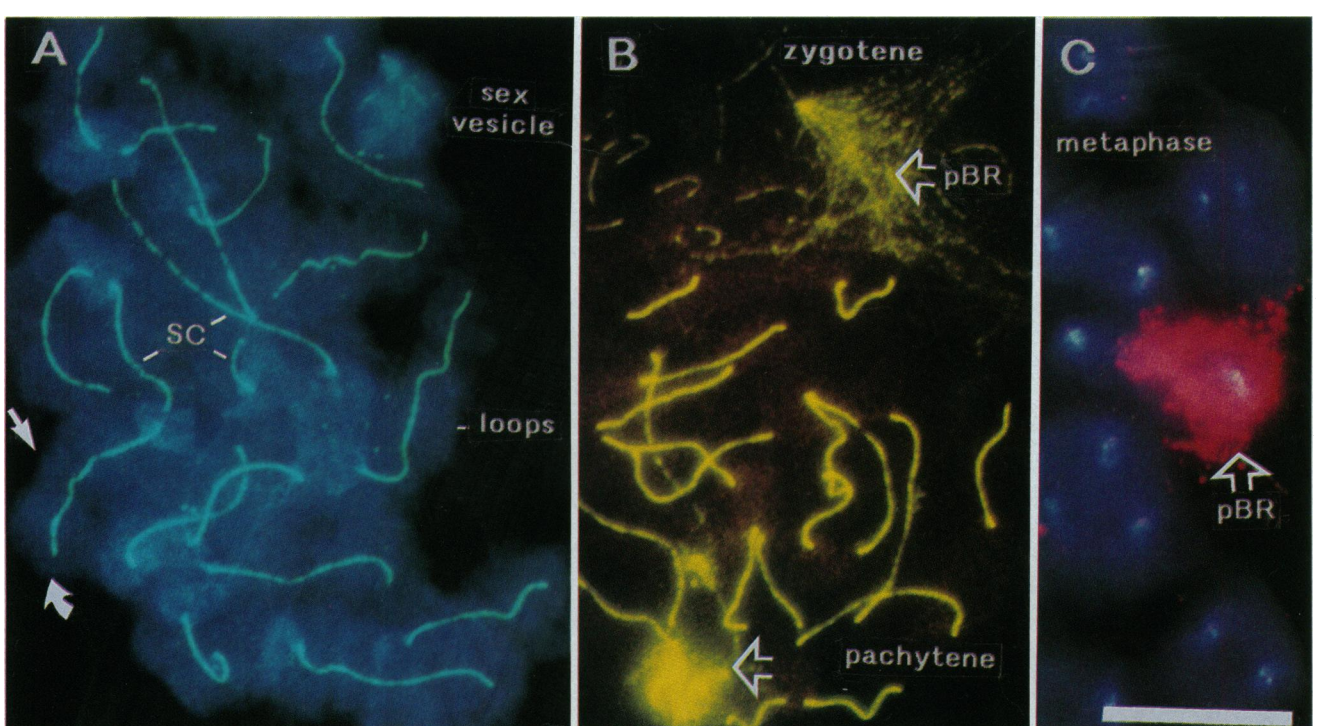

FIG. 1. Comparison of degree of chromatin loop compaction during various stages of meiosis. (*A*) Whole-mount surface spreads of meiotic nuclei were immunostained with anti-synaptonemal complex (SC) antibodies and subsequently subjected to FISH. Such nuclei illustrate that the chromatin loops which form around a proteinaceous core, the SC, during meiotic prophase vary in loop size relative to their chromosomal position. *(A)* In this DAPI-stained nucleus, loops located at the ends of the chromosome (curved arrow) are shorter than those found interstitially (straight arrow). *(B)* This picture contains two nuclei, one in zygotene, the other in pachytene. Their protein cores are stained with antibody against the SC core protein, cor1, and visualized in yellow with FITC. Foreign inserts such as pBR-globin (a bacterial–human hybrid sequence) (open arrows) are unable to undergo packaging in concert with the native chromatin. The direct comparison of the degree of compaction shown in this micrograph indicates that the pBR loops, which are highly dissociated at zygotene, reach their maximum condensation at pachytene. *(C)* This condensation relaxes somewhat at metaphase I, but not to the zygotene levels. (Bar = 10 μm.)

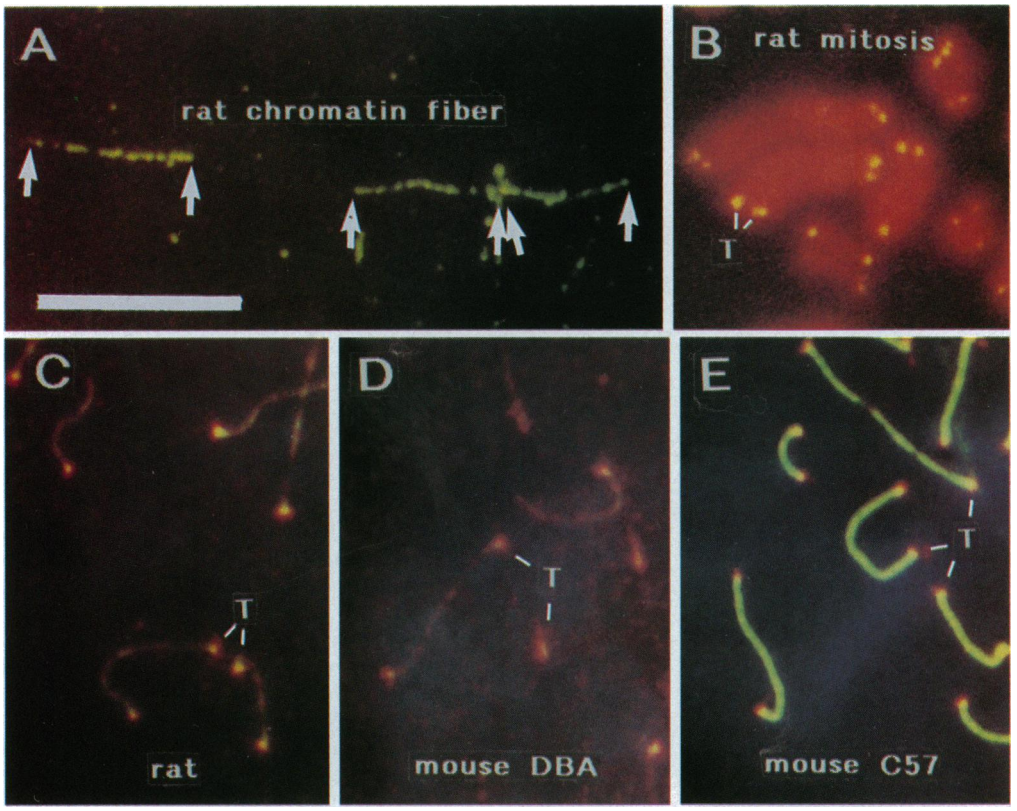

FIG. 2. Comparison of telomere FISH signals of different species and different chromatin formats. (*A*) Arrows mark three FISH-highlighted telomeres of three different chromatin fibers of a rat nucleus. (*B*) The rat telomere FISH signal (T) in mitotic metaphase is virtually identical in size to that in pachytene (*C*). (*C–E*) In these three pachytene nuclei, there is little difference in FISH signal between the 78-kb rat and mouse lines DBA (67 kb) (*D*) and C57 (40–50 kb) (*E*) in spite of their considerable differences in telomere length. (Bar = 10 μm.)

structures resulting in variation in insert size and chromosomal location. The copy number of each strain's insertion was initially estimated by Southern blot analysis and the approximate number of integrated chromosome copies per cell was 20–40 (lines 47 and 50), 15–30 (line 18A), and 5–10 (line 30).

These estimates of copy number were determined more precisely by measurement of FISH signals on released chromatin fibers (10, 11, 13). The 40 kb of Cos 165-1, the cosmid probe used as an internal standard, occupied 12.5 ± 0.8 μm detected by FISH on chromatin fibers. Fiber mapping generated the following data: line 47, 30 copies; line 50, 15–20 copies; line 18, 20 copies; line 30, 5–10 copies (Table 2).

When nontelomeric sequences were transposed toward the end of the chromosome, chromatin packaging decreased the loop size from 5.5 to 1.5 μm as the insert moved closer to the end of the chromosome (Fig. 4*A*). The 110-kb insert of transgenic line 18A located interstitially formed 5.5-μm loops, similar to the surrounding chromatin (Fig. 4*B*). Line 50's 95-kb insert was within 1 μm from the chromosome end and formed loops of 4.5 μm (Fig. 4*C*), a reduction of 29% of the interstitial loop length. Line 47, the longest insert at 160 kb and located ≈0.3 μm from the chromosome tip, had a loop of 2 μm (Fig. 4*D*), a reduction of 52% of the interstitial length. Finally, in line 30 the sequence inserted at the proximal end of the telomere

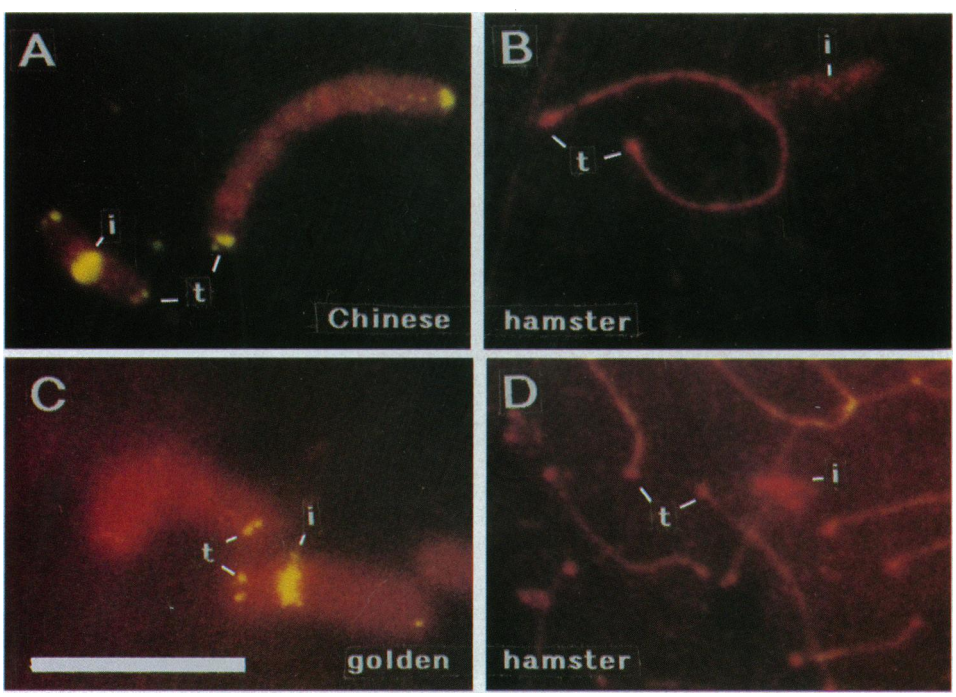

FIG. 3. Hamster telomere FISH signals. In both the Chinese (*A* and *B*) and golden hamster (*C* and *D*) FISH signals of the terminal telomeres (t) are similar to those of rat and mouse. However, when this sequence relocates interstitially (i), the condensed signal disappears and the telomere sequences form loops of similar size to the adjacent sequences. Telomeric sequences were detected by FISH both at metaphase (*A* and *C*) and at pachytene (*B* and *D*). (Bar = 10 μm.)

Table 1. Telomere characteristics of various species

Species	Total length, μm	Estimated kb	Average copy no. (6-bp repeat of TTAGGG)	Morphology
Mouse C57	10.27 ± 5.88	33	6,300 ± 800	Short loops
Mouse DBA	19.62 ± 5.59	67	10,100 ± 934	Short loops
Rat	24.09 ± 6.41	78	13,000 ± 1068	Short loops
Hamster	8.99 ± 3.17	29	5,200 ± 300	Short loops

region. Its loops were 1.5 μm (Fig. 4*E*), a decrease of 74% of the interstitial length. The 30-kb insertion size of line 30 was smaller than a telomere sequence. However, it formed measurable loops as opposed to the condensed FISH signal of the terminal telomere. In addition, the behavior of the line 30 insert strongly suggested that a 50- to 100-kb telomeric sequence would be sufficient to form visible loops if it was located in other than a terminal position. These data, summarized in Table 2, show that the reduction in loop length was not simply a function of insert size.

For comparison, mouse major and minor satellite DNA probes were also used to measure the loop size for both sequences on mouse meiotic chromosomes. Their data are presented in Fig. 4*E*. Interestingly, the minor satellite sequences form much smaller loops than the major satellite. This correlates with the data on the insertion sequences as the minor satellite sequences are located closer to the telomere than the major satellite.

DISCUSSION

Role of Sequence/Position in Chromatin Packaging. Our transgenic experiments clearly show that there is a separate chromatin packaging regulation mechanism which operates in the telomeric region. One possibility is that the telomeric sequence itself is intricately linked to this mechanism. However, when these sequences are relocated away from the terminus of the chromosome, such as the interstitial TTAGGG sequences of the hamster, they escape the small loop regulation and form the larger loops common to the interior of the chromosome. This observation further demonstrates that the key factor for forming small loops is related to the telomeric region rather than to the TTAGGG sequence.

While our data indicate a dominant role for chromosomal position in regulation of chromatin packaging, one must not overlook the contribution of DNA sequence to this process. Previous studies have demonstrated the necessity for certain

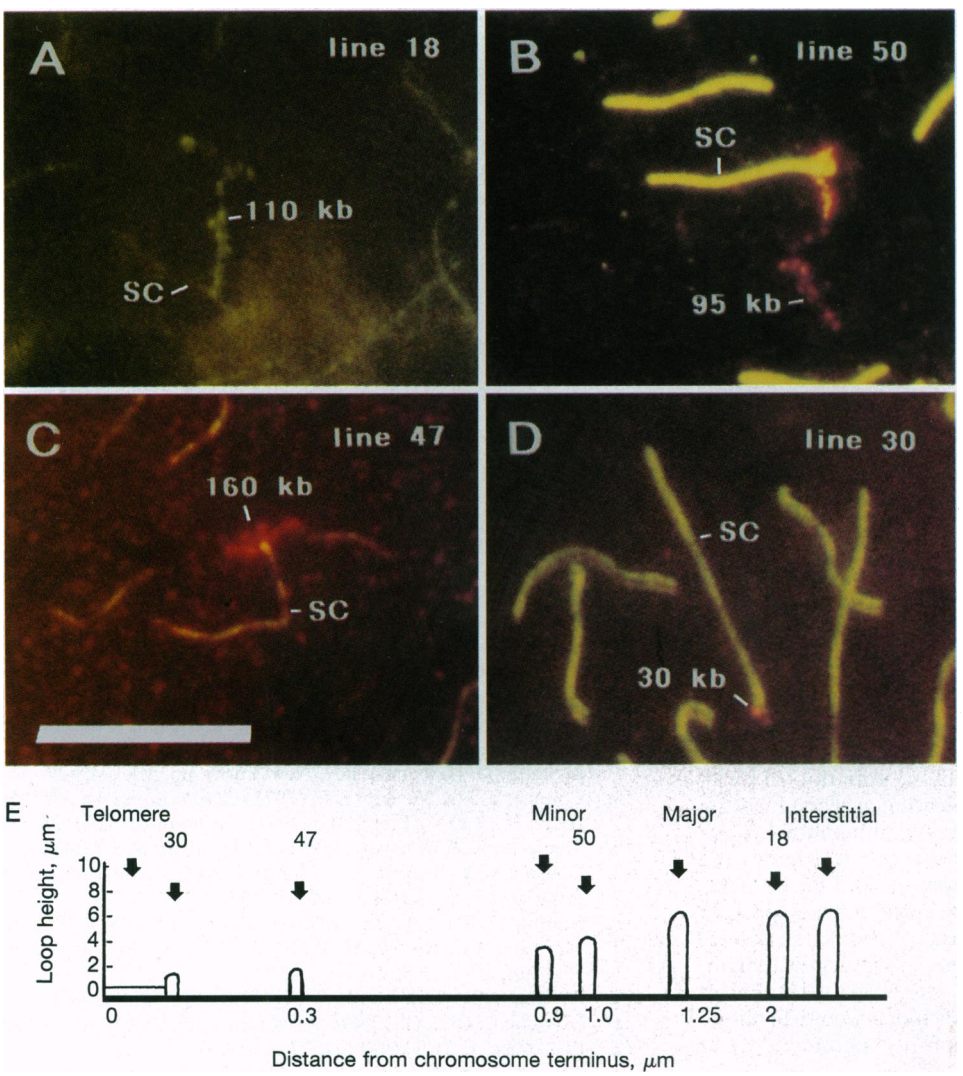

FIG. 4. Loop size of interstitial sequences varies according to distance from the chromosome end. (*A*) The interstitially positioned 110-kb insert of line 18 forms loops of equivalent length to the surrounding chromatin. (*B*) Inserted 1 μm from the telomere, the 95-kb insert of line 50 diminishes to an average loop length of 4.5 μm. (*C*) The longest insert, the 160 kb of line 47, is even closer to the telomere at 0.3 μm. This is sufficient to cause the loops to shrink to 2 μm. (*D*) The distance of the 30-kb insert of line 30 is too close to the telomere to be measured. Its 1.5-μm loops are slightly larger than the unmeasurable signal of the telomere. (*E*) While not all the inserts occur on the same chromosome of the four transgenic mouse lines, *E* is a schematic diagram showing the relative positions of the inserts with respect to the distance from the chromosome end. Also shown are the relative loop lengths of the inserts as well as the major and minor satellites. Here, "interstitial" refers to interstitial telomeric loops.

Table 2. Characteristics of transgenic mouse lines, detailing insert length in terms of loop length, numbers of kilobases, and distance from terminal telomere

Mouse C57 transgenic line	Insert length, μm	Estimated kb	Copy no.	Distance from telomere, μm	Average loop size, μm
C57, line 18	37.5 ± 8.42	100–120	17–20	1.93 ± 0.49	5.54 ± 1.78
C57, line 30	7.95 ± 3.09	26–32	4–5	Adjacent	1.47 ± 0.28
C57, line 47	61.25 ± 15.49	150–180	25–31	0.29 ± 0.05	2.09 ± 0.65
C57, line 50	31.88 ± 8.67	90–100	15–17	0.96 ± 0.27	4.47 ± 2.0

sequence or DNA modifications in order to form species-specific sized loops (6).

In the case of loop size of the interstitial telomere sequences, one might argue that the increased loop size was due to the increased number of telomere repeats in the interstitial versus the terminal position. However, as shown by the behavior of the virtually telomeric insert 30, there exists enough $(TTAGGG)_n$ DNA at the ends of the chromosomes to form loops. Coupled with the observation of loop formation in lines 18 and 47, it is unlikely that the number of telomeric repeats is exclusively responsible for the variation in the degree of condensation between the intra- and terminal chromosomal positions. This may be clarified in the future by observing the behavior of smaller $(TTAGGG)_n$ repeats in the nontelomeric region.

It is likely that at least two regulatory mechanisms exist for packaging meiotic chromatin into loops. Sequence determines the potential for loop formation, while the size of the loop is controlled by chromosome position. Since both telomeric and nontelomeric sequences are processed in a similar fashion dependent on their chromosomal position, the implication is that there exists at least one packaging mechanism not dependent on sequence. However, it is yet to be established whether all interstitial loops are the same size or whether there is variation among interstitial loops at different stages of meiosis.

One may speculate on the nature of the regulatory mechanisms that allow interstitially located telomere sequences to adopt the packaging pattern of nonterminal nucleotides. One hypothesis is that chromatin is bound into tight loops by packaging proteins only at the terminus of the chromosome. Interstitially, the folding is a result of crumpling of the chromatin imposed by the restriction of the nuclear volume (E. Siggia and J. Marks, personal communications). Alternatively, both interstitial and terminal packaging may be the result of different packaging proteins.

The involvement of protein in chromatin packaging is well known. For example, removing histones from mitotic chromosomes results in the decondensation of chromatin loops (20). Furthermore, our studies indicate that specific parts of the chromosome may have their own protein components. In fact, the DNA–protein interaction pattern of nucleosomes is distinctive in the terminal versus the interstitial regions (7, 8). Therefore, it is reasonable to speculate that this regional differential also holds true for high-order structure formation.

Possible Role of Differential Chromatin Packaging. The conservation in chromosome end packaging suggests a critical role for this differential chromatin organization. The unique properties of the chromosome ends are thought to play a role in gene expression, nuclear organization, initiation of chromosome pairing in meiosis, and modification of recombination frequencies (8, 21, 22). Rates of genetic recombination in male humans and mice are very high near the telomeric and subtelomeric regions of the chromosome (23). Our observation of smaller chromatin loops at the terminus may provide some mechanical basis to explain these phenomena. Besides the obvious role of end stabilization, it is possible that increased rates of recombination are correlated to the shorter loop lengths in this region since such loops would facilitate pairing of homologous sequences of nonsister chromatids at or near the synaptonemal complex.

The recognition of distinct regions of morphology on the eukaryotic chromosome has led to appreciation of the chromosome as an organelle with differential and reversible functions during the life of the cell. Our study adds to this collection of information, illustrating that the species-specific sized loops that form around a protein core during meiosis vary dramatically in size depending on their chromosomal position. In addition, the packaging mechanism in the terminal region of the chromosome appears highly conserved since virtually every species tested had a tightly condensed FISH signal at terminally located telomeres. This intrachromosomal regulation of loop size seems more likely due to proteins rather than to specific DNA sequences. The significance of this differential packaging remains to be elucidated; however, it suggests that there exists a chromosome packaging mechanism common to many eukaryotes.

This research was supported by grants from the Natural Science and Engineering Research Council of Canada to P.B.M. and the Medical Research Council of Canada to L.-C.T. H.H.Q.H. is supported by a Natural Science and Engineering Research Council of Canada postdoctoral fellow award.

1. Weith, A. & Traut, W. (1980) *Chromosoma* **78,** 275–291.
2. Moens, P. B. & Pearlman, R. E. (1989) *Chromosoma* **98,** 287–294.
3. Li, S., Meistrich, M. L., Brock, W. A., Hsu, T. C. & Kuo, M. T. (1983) *Exp. Cell Res.* **144,** 63–67.
4. Pearlman, R. E., Tsao, N. & Moens, P. B. (1992) *Genetics* **130,** 865–872.
5. Moens, P. B. & Pearlman, R. E. (1990) *Chromosoma* **100,** 8–14.
6. Heng, H. H. Q., Tsui, L.-C. & Moens, P. B. (1994) *Chromosoma* **103,** 401–407.
7. Makarov, V. L., Lejnine, S., Bedoyan, J. & Langmore, J. P. (1993) *Cell* **73,** 775–787.
8. Tommerup, H., Dousmanis, A. & De Lange, T. (1994) *Mol. Cell. Biol.* **14,** 5777–5785.
9. Chamberlain, J. W., Nolan, J. A., Vasavada, H. A., Vasavada, H. H., Ploegh, H., Ganguly, S., Janeway, C. A., Jr., & Weissman, S. M. (1988) *Proc. Natl. Acad. Sci. USA* **85,** 7690–7694.
10. Heng, H. H. Q., Squires, J. & Tsui, L.-C. (1992) *Proc. Natl. Acad. Sci. USA* **89,** 9505–9513.
11. Fidlerova, H., Senger, G., Kost, M., Sanseau, P. & Sheer, D. (1994) *Cytogenet. Cell Genet.* **65,** 203–205.
12. Heng, H. H. Q. & Tsui, L.-C. (1994) in *Methods in Molecular Biology: In Situ Hybridization Protocols*, ed. Choo, K. H. A. (Humana, Clifton, NJ), pp. 109–122.
13. Heng, H. H. Q., Tsui, L.-C., Windle, B. & Parra, I. (1995) in *Current Protocols for Human Genetics*, eds. Dracopoli, N., Haines, J., Korf, B., Moir, D., Morton, C., Seidman, C., Seidman, J.-G. & Smith, D. (Greene-Wiley, New York), pp. 4.5.1–4.5.26.
14. Counce, S. J. & Meyer, G. F. (1973) *Chromosoma* **44,** 231–253.
15. Heng, H. H. Q. & Tsui, L.-C. (1993) *Chromosoma* **102,** 325–332.
16. Moens, P. B. & Moens, T. (1981) *J. Ultrastruct. Res.* **75,** 131–141.
17. Dobson, M. J., Pearlman, R. E., Karaiskakis, A., Spyropoulos, B. & Moens, P. B. (1994) *J. Cell Sci.* **107,** 2749–2760.
18. Kipling, D. & Cooke, H. (1990) *Nature (London)* **347,** 400–402.
19. Meyne, J., Goodwin, E. H. & Moyzis, R. K. (1990) *Chromosoma* **99,** 8–14.
20. Paulson, J. R. & Laemmli, U. K. (1977) *Cell* **12,** 817–828.
21. Gottschling, D. E. (1992) *Proc. Natl. Acad. Sci. USA* **89,** 4062–4065.
22. Blackburn, E. H. (1994) *Cell* **77,** 621–623.
23. Ashley, T. (1994) *Hum. Genet.* **94,** 587–593.